

Supplemental material

Shi et al., <https://doi.org/10.1084/jem.20190980>

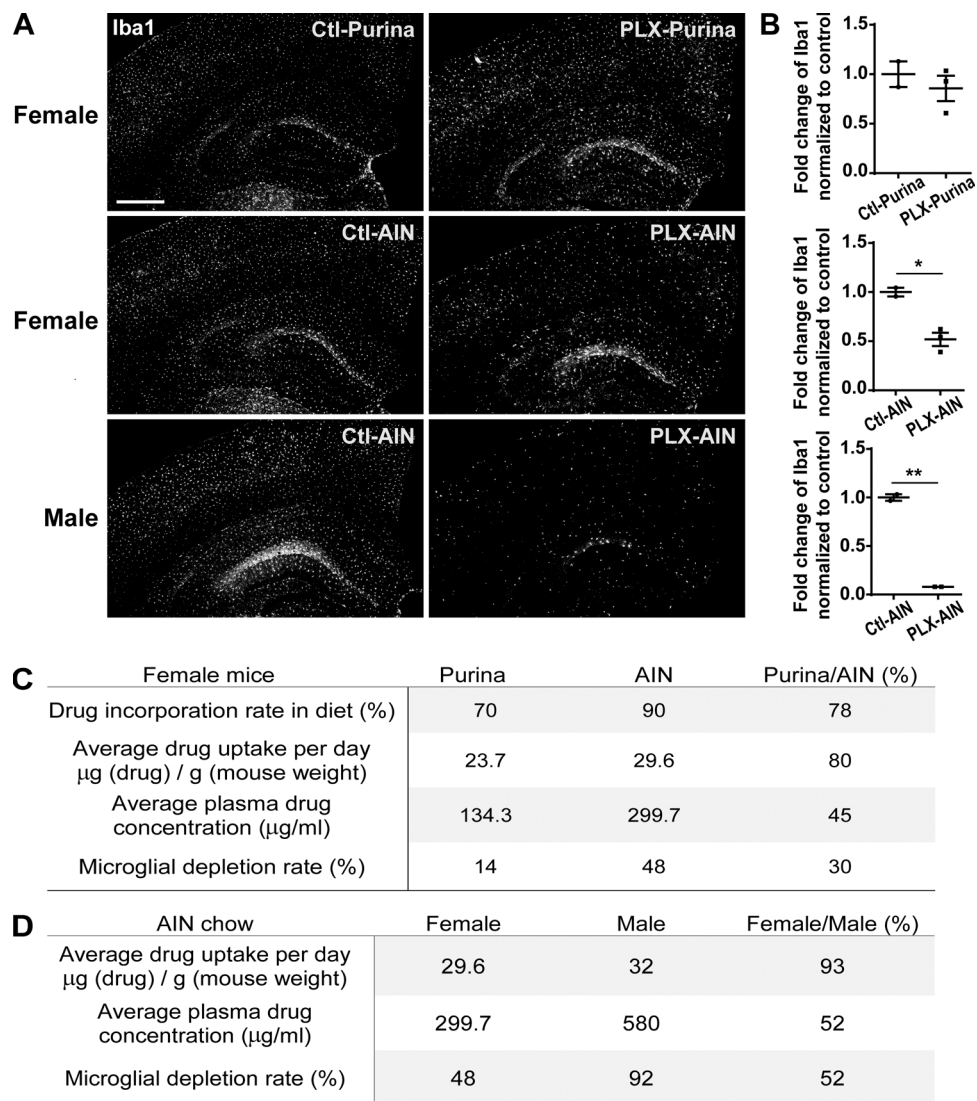


Figure S1. **Mouse sex and chow formula impact the efficiency of microglial depletion by PLX3397.** (A) Iba1 staining images for 3–4-mo-old female or male TE4 mice treated with 300 mg/kg PLX3397 supplemented in either Purina-5053 or AIN-76A diet for 7 d ($n = 2-3$ mice per group). Scale bar = 500 μm for all images. (B) Quantification of Iba1-covered area in the hippocampus. (C and D) Effects of chow formula and sex on serum PLX3397 levels in relation to microglial depletion rate. Data are expressed as means \pm SEM. One-way ANOVA with Tukey's post hoc test. *, $P < 0.05$; **, $P < 0.01$. The experiments in A and B were repeated three times.

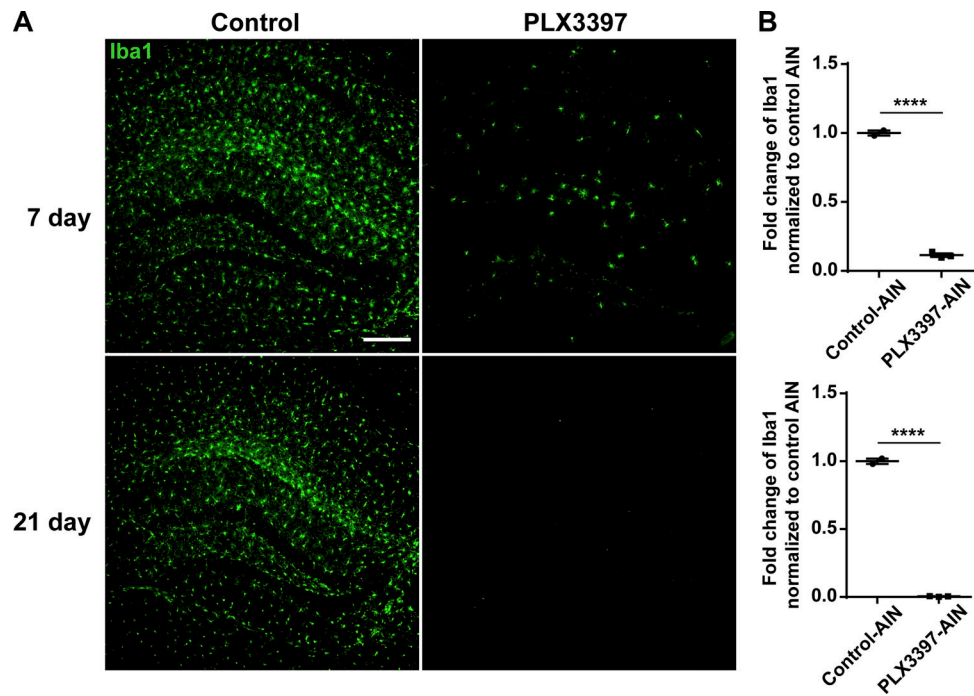


Figure S2. **PLX3397 supplemented in the AIN-76A diet at 400 mg/kg chow depletes microglia with high efficiency.** (A) Iba1 staining images for 5–6-month old male E4 mice treated with 400 mg/kg PLX3397 supplemented in the AIN-76A diet for 7 or 21 d ($n = 2-3$ mice per group). Scale bar = 200 μm for all images. (B) Quantification of Iba1-covered area in the hippocampus. Data are expressed as means \pm SEM. One-way ANOVA with Tukey's post hoc test. ****, $P < 0.0001$. This characterization experiment was performed once.

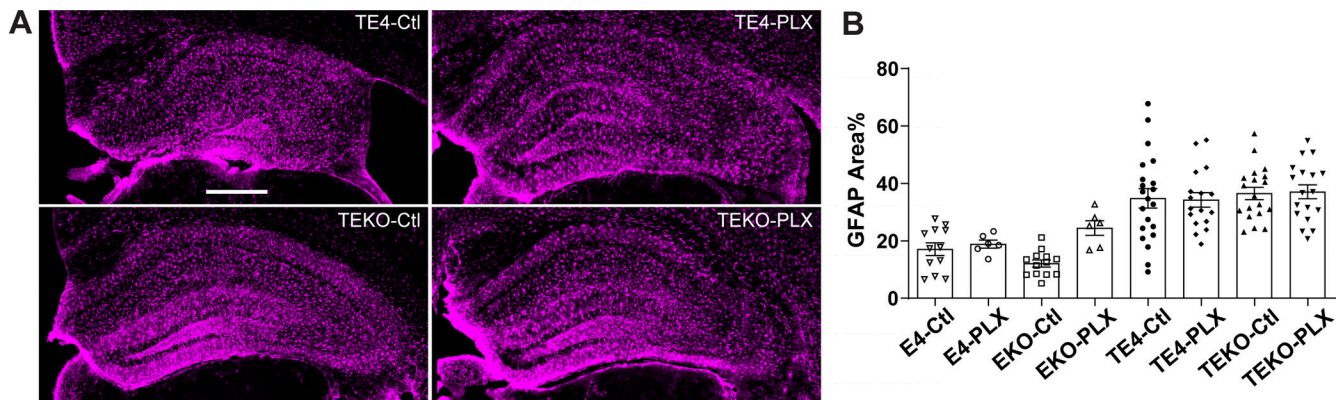


Figure S3. **PLX3397 treatment does not affect GFAP⁺ astrocytes.** (A) Representative images of GFAP staining for 9.5-month old TE4 and TEKO mice treated with control (Ctl) or PLX3397-supplemented (PLX) chow. Scale bar = 500 μm for all images. (B) Quantification of GFAP-covered area in the hippocampus of all mice (TE4-Ctl: $n = 21$; TE4-PLX: $n = 17$; TEKO-Ctl: $n = 19$; TEKO-PLX: $n = 18$; E4-Ctl: $n = 12$; E4-PLX: $n = 6$; EKO-Ctl: $n = 13$; EKO-PLX: $n = 6$). Data are expressed as means \pm SEM. One-way ANOVA with Tukey's post hoc test. The GFAP staining was performed once.

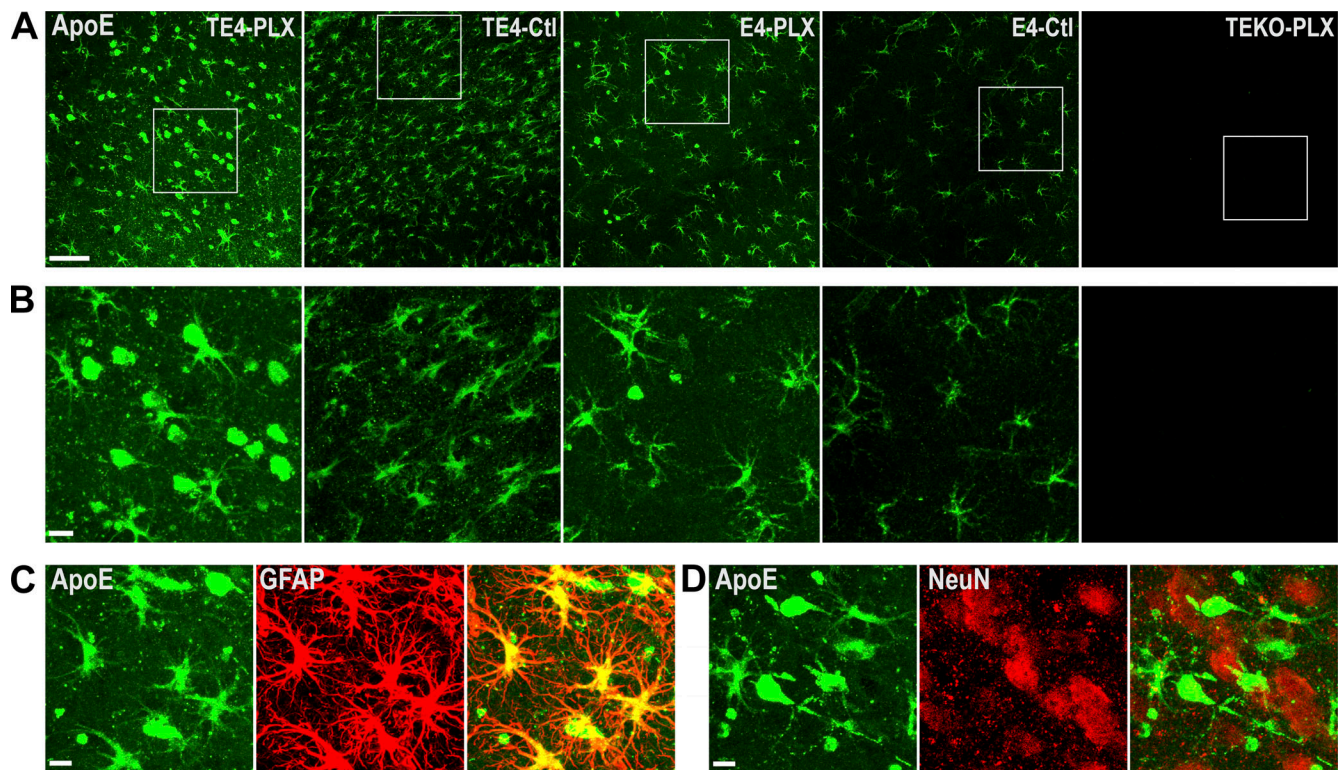


Figure S4. **ApoE is elevated in astrocytes and neurons in the piriform/entorhinal cortex of PLX3397-treated TE4 and E4 mice.** (A) Representative images of apoE staining in the piriform/entorhinal cortex of 9.5-mo-old TE4-PLX, TE4-Ctl, E4-PLX, E4-Ctl, and TEKO-PLX mice, respectively. Scale bar = 50 μ m for all images. (B) Zoom-in of the selected area in A. Scale bar = 10 μ m for all images. (C) Co-localization of apoE with GFAP⁺ astrocytes in the piriform/entorhinal cortex of TE4-PLX mouse. Scale bar = 10 μ m. (D) Non-co-localization between apoE and NeuN in the piriform/entorhinal cortex of TE4-PLX mouse. Scale bar = 10 μ m. ApoE staining was repeated seven times using different antibodies.

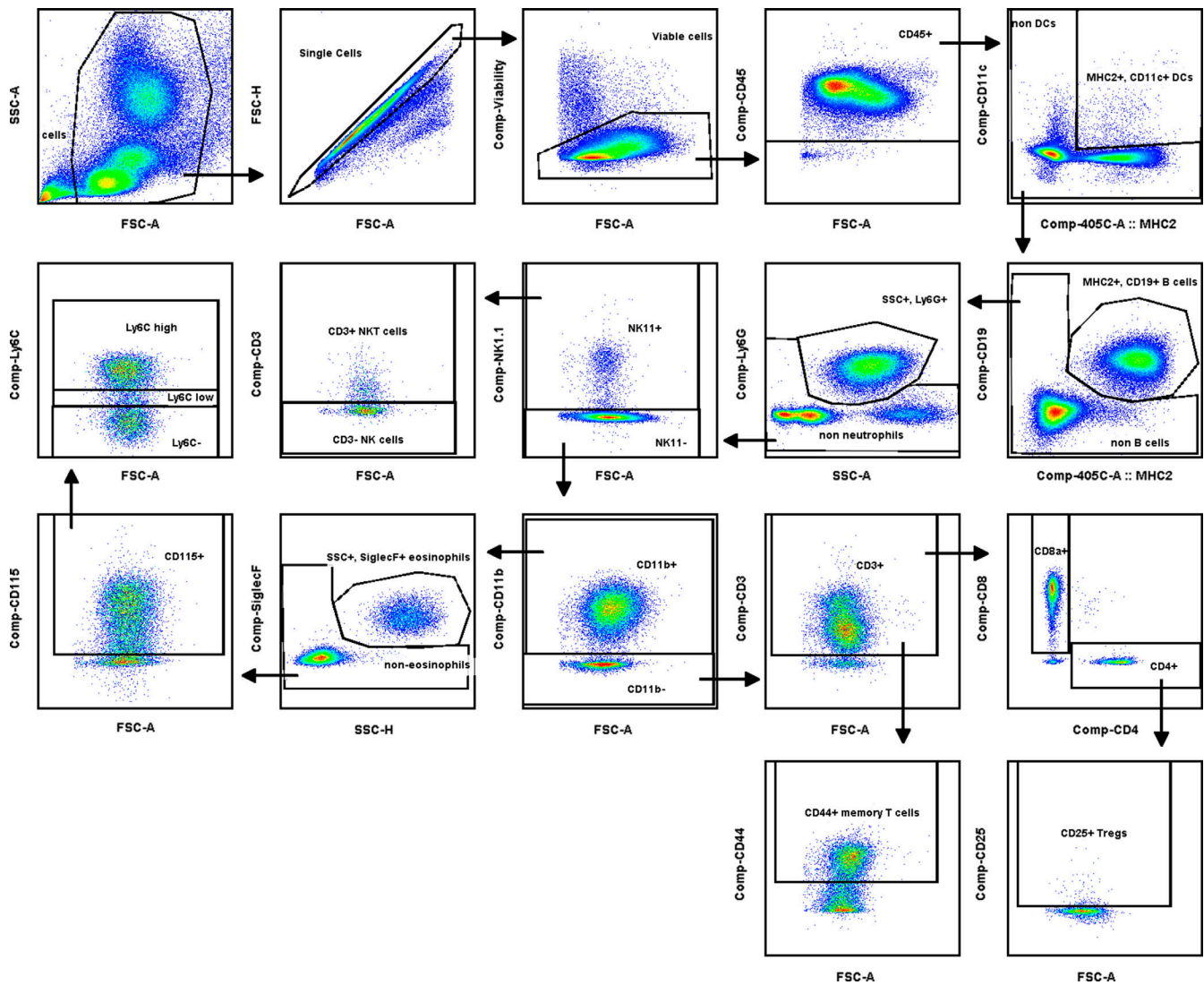


Figure S5. **Gating strategies for isolating blood cell types using flow cytometry.** Blood cells were sequentially gated through total cells, single cells, viable cells, and CD45⁺ cells. From the CD45⁺ gate, DCs were isolated as the MHC2⁺CD11c⁺ population. From the non-DC gate, B cells were isolated as the MHC2⁺CD19⁺ population. From the non-B cell gate, neutrophils were isolated as the SSC^{high}Ly6G⁺ population. From the nonneutrophil gate, NK1.1⁺ cells were isolated and further divided into CD3⁺ NK T cells and CD3⁻ NK cells. The NK1.1⁻ gate was further separated into CD11b⁺ and CD11b⁻ gates. From the CD11b⁺ gate, eosinophils were isolated as the SSC^{high}SiglecF⁺ population. From the noneosinophil gate, monocytes were isolated as the CD115⁺ population, which was further divided into Ly6C^{hi}, Ly6C^{lo}, and Ly6C⁻ populations. From the CD11b⁻ gate, T cells were isolated as the CD3⁺ population, which was further separated into CD4⁺ and CD8⁺ T cells, or CD44⁺ memory T cells. From the CD4⁺ T cell gate, T reg cells were isolated as the CD25⁺ population. SSC-A, side scatter area; FSC-A, forward scatter area; SSC-H, side scatter height.